INTERNATIONAL JOURNAL OF INTEGRATED ENGINEERING
ISSN: 2229-838X e-ISSN: 2600-7916

IJIE

Vol. 16 No. 1 (2024) 282-292
https://publisher.uthm.edu.my/ojs/index.php/ijie

An Ultra-Wideband Antenna with Triple Band-Notched Characteristics for Wearable Application

M. A. A. Rashid[1], S. M. Shah[2]*, H. A. Majid[2], U. Musa[2], N. S. Suriani[3]

[1] *Avery Dennison Smartrac, Kulim, Kedah, 09000, MALAYSIA*
[2] *Advanced Telecommunication Research Center (ATRC), Universiti Tun Hussein Onn Malaysia, Parit Raja, Johor, 86400, MALAYSIA*
[3] *Faculty of Electrical and Electronic Engineering, Universiti Tun Hussein Onn Malaysia, Parit Raja, Johor, 86400, MALAYSIA*

*Corresponding Author: shaharil@uthm.edu.my
DOI: https://doi.org/10.30880/ijie.2024.16.01.023

Article Info

Received: 16 November 2023
Accepted: 18 April 2024
Available online: 22 May 2024

Keywords

Ultra-wideband, triple band-notched, worldwide interoperability for microwave access (WiMAX), wireless local area network (WLAN), specific absorption rate (SAR)

Abstract

This work presents a compact UWB antenna with triple band-notched at WiMAX (3.2 GHz to 3.7 GHz), C-band (3.7 GHz to 4.2 GHz) and WLAN (5.15 GHz to 5.35 GHz) for wearable applications. The UWB antenna is fabricated on a semi-flexible thin FR-4 substrate. In order to reduce the complexity, only two slots are introduced on the radiating patch instead of three slots to reject each narrowband frequency. In this case, one slot rejects a combination of WiMAX and C-band and the other slot rejects the WLAN frequency band. The UWB antenna on the thin FR-4 material has an overall size of 21×16 mm2, which is very compact and thus, suitable for wearable applications without causing discomfort when worn on-body. Although the antenna is small in size, the performance is not compromised. The UWB antenna has the frequency range from 2.51 GHz to 12.09 GHz, maximum radiation efficiency of 100% and maximum gain of 4 dBi. Nevertheless, the antenna is able to reject the WiMAX and C-band as well as the WLAN band. The simulated specific absorption rate (SAR) results show that the antenna complies with the SAR limit Federal Communication Commission (FCC) and International Commission of Non-Ionizing Radiation Protections (ICNIRP) standards for 1 mW input power. Bending investigations performed on different diameters of Styrofoam cylinders shows that the frequency range and the notch bands are not very much affected.

1. Introduction

Applications based on ultra-wideband (UWB) technology have achieved considerable development due to their appealing characteristics, such as low power consumption, high speed transmission rate and ability to prepare for short range wireless communication links that use low-cost and low-energy transmitter or receiver; wearable body area network (WBAN) is among the most attractive application [1]. A wearable antenna is a key component for the WBAN network as it is responsible for transmitting and receiving the signal between the implantable device (such as pacemakers, heart rate monitors, and respiratory monitor) and wearable network [2],[3]. Furthermore, the wearable antenna is critical for a proper operation of the WBAN system as it can be placed on a human body and thus, the influence of the human on the characteristics of the antenna should be taken into account during the initial design stage [4].

An important consideration for UWB antennas is the strong interference from the existing wireless network technologies, for instance, wireless interoperability for microwave access (WiMAX) between 3.2 GHz to 3.7 GHz and C-band between 3.7 GHz to 4.2 GHz [5]–[7]. Besides, according to the IEEE 802.11a standard, for an UWB antenna to work in wearable and indoor applications, it should avoid the higher frequency band from 5.15 GHz to 5.35 GHz which is assigned for Wireless Local Area Network (WLAN) [8]. These three bands may cause interference and thus reduce the performance of UWB antennas. As a result, it is appropriate to notch the unwanted frequency bands that are susceptible to strong interference within the UWB frequency range. Specific Absorption Rate (SAR) is an established mechanism for measuring the electromagnetic energy absorbed by biological tissue when exposed to radiated electromagnetic energy from an antenna [9]. The SAR limit set by the Federal Communication Commission (FCC) is 1.6 W/kg averaged over 1 g of actual tissue while the SAR limit recommended by the International Commission on Non-Ionizing Radiation Protection (ICNIRP) is 2.0 W/kg averaged over 10 g of actual tissue [10]. Influence of body proximity on the performance of antennas and the amount of SAR absorbed by the human body are the two significant on-body measurements for wearable antennas.

Introducing resonant structures on the radiating patch or feed line has been attempted to notch the unwanted narrowband [11],[12]. Stubs loading onto the antenna structure is a frequently used technique for incorporating notch bands into wideband antennas. Loading the stubs on the radiating patch or ground plane in quadrature transfuses the fundamental frequencies and harmonics, thereby obliterating the intended notch band of frequencies [13]. Other methods have also been used such as by etching various shapes of slots on the radiating patch and/or on the ground, adding folded parasitic strips or resonators in the vicinity of the radiating or the feed line and multiple other techniques. Each notch structure can only reject one unwanted band. Therefore, to yield multiple notched bands, multiple notch structures are necessary. This in return, will introduce complexity to the antenna's design and configuration.

Hence, an UWB antenna with triple band-notch characteristics is proposed in this work to alleviate the potential EM interference arises from the narrow band applications. The band-notched operations are achieved by etching slots in the rectangular metal radiating patch [14]. The designed antenna is compact in terms of the size which is 21 × 16 mm2 and is fabricated on a thin FR-4 substrate material to ensure flexibility. The highly compact size of the antenna not only caters to the need of a compact size antenna to support multiple applications but is also particularly useful for wearable applications if the antenna is to be worn on the body.

2. Methodology

This section explains the method used in order to obtain the results of the work, including the design stage and the simulation stage that are performed by using CST MWS® software. Four UWB antennas on FR-4 substrate are designed, presented and analyzed in this work:

Four UWB antennas on FR-4 substrate are designed, presented and analyzed in this work:

- Fundamental UWB antenna (UWB-FR4)
- UWB antenna with first slot to notch the WiMAX and C-band (UWB-FN-FR4)
- UWB antenna with second slot to notch the WLAN band (UWB-SN-FR4)
- UWB antenna with combination of two slots to notch the WiMAX, C- and WLAN bands (UWB-TN-FR4)UWB Antenna with Rogers Duroid RO3003™ Substrate

The proposed UWB antenna with rogers duroid substrate can be seen in Fig. 1 with top view and bottom view. The radiating patch at the top view is from copper material with a thickness of 0.035 mm. The substrate of this simulation antenna is using Rogers Duroid RO3003™ with a dielectric constant, εr of 3, loss tangent, tan δ of 0.010 and thickness, h of 1.52 mm. The ladder shape and a rectangular slot on the radiating patch are introduced to improve the impedance bandwidth of the antenna.

2.1 The Fundamental UWB-FR4 Antenna Design

The initial UWB-FR4 antenna design started with a simple rectangular patch antenna design adopted from [15]. According to the paper, the UWB antenna has a size of 17.5 × 20.5 mm2. However, it is designed on a rigid and thick FR-4 substrate of 1.6 mm. In this work, instead of using two ladder steps, only one ladder step is introduced at the two corners of the bottom edge of the radiating patch in order to improve the bandwidth performance and reduce simulation time. The antenna has been optimized to operate within the UWB frequency range from 3.1 GHz to 10.6 GHz. The proposed UWB-FR4 antenna in this work can be seen in Fig. 1 and the dimensions of the antenna are listed in Table 1. From the figure, the antenna consists of a rectangular radiating patch with a microstrip feed line. The radiating patch and ground plane are made up of copper with a thickness of 0.035 mm. The substrate of the antenna is FR-4 material with a dielectric constant, εr of 4.5, loss tangent, tan δ

Int. Journal of Integrated Engineering Vol. 16 No. 1 (2024) p. 282-292

of 0.019 and thickness, h of 0.5 mm. A slot is embedded on the partial ground plane so that the impedance bandwidth of the antenna can be further increased. This UWB-FR4 antenna has a compact size of 16 × 21 mm².

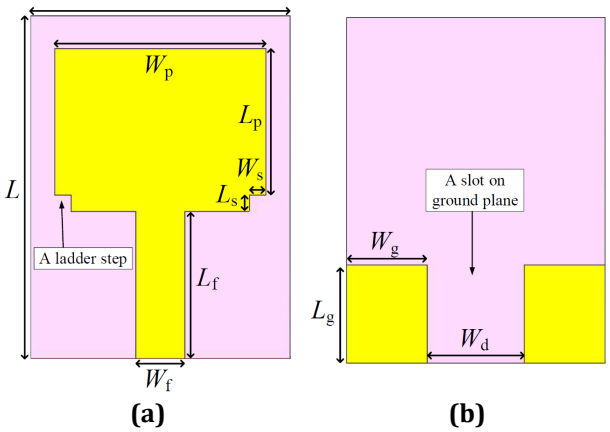

Fig. 1 *The proposed UWB-FR4 antenna (a) Top view; (b) Bottom view*

Table 1 *Dimensions of the fundamental UWB-FR4 antenna*

Parameter	Values (mm)
L	16
W	21
L_p	9
W_p	13
L_f	9
W_f	3
L_g	5
W_g	5
L_s	1
W_s	1
W_f	6

2.2 Design and Configuration of the UWB Antenna with Notch Bands

In order to achieve an UWB antenna with band notch characteristics, a first slot is introduced on the radiating patch to simultaneously reject the WiMAX and C-bands. The second slot is introduced to notch the WLAN band. At the final stage, both slots are combined into a single UWB antenna to reject the three narrowband applications. The evolution of the antennas can be viewed in Fig. 2.

2.2.1 UWB-FN-FR4 Antenna

The design approach for UWB-FN-FR4 antenna with the first slot to notch the WiMAX and C- bands are discussed in this section. Due to the fact that the WiMAX and C-band frequencies bands are close neighbors, only one slot on the radiating plane is used to notch both bands. This reduces the complexity and simplifies the fabrication process. The notched bands are obtained by embedding an inverted L-shaped slot on the radiating patch of the UWB-FR4 antenna [16], [17]. Fig. 2 (a) represents the geometry of the proposed UWB-FN-FR4 antenna with the first and second band-notched characteristics. The slot is responsible for introducing rejection of interfering signals from WiMAX (3.2 GHz – 3.7 GHz) and C-band (3.7 GHz – 4.2 GHz) narrowband communication systems. The slot's initial length has been calculated to a quarter wavelength (λg/4) at center frequency 3.7 GHz [18]. In addition to the length of the slot, the width and location of the slot may also shift the rejection bands. The slot is placed at the upper region of the radiating plane to obtain the desired notch centered at 3.7 GHz.

2.2.2 UWB-SN-FR4 Antenna

In order to reject the 5.15 GHz to 5.35 GHz band that overlaps with the lower band WLAN [19], a second slot is added on the radiating patch. The slot in Fig. 2 (b) has a total length of 30.6 mm; approximately λg/2 at 5.25 GHz which is the WLAN band center frequency. The slot operates like a band notch filter with the length of a half wavelength. A parametric study is carried out in order to determine the best position and dimensions for the second slot to notch the WLAN band.

2.2.3 UWB-TN-FR4 Antenna

The UWB-TN-FR4 antenna with triple notch bands characteristic is achieved by combining the first slot for WiMAX and C-band rejection and the second slot for WLAN band rejection. The dimensions of the slots are further optimized with a parametric study to produce an UWB-TN-FR4 antenna that rejects WiMAX, C-band and WLAN bands. Fig. 2 (c) illustrates the design of the UWB-TN-FR4 antenna with the WiMAX, C- and WLAN bands rejection. The dimensions of the optimized slots are shown in Table 2. One of the main attractive features of this

proposed UWB-TN-FR4 antenna with triple notched-band characteristics is its small size to cater to the need for wearable application. This antenna has a compact dimension of 21×16 mm².

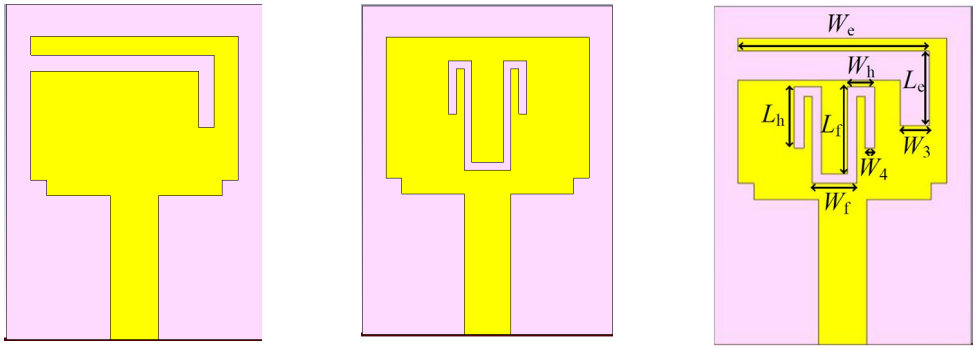

Fig. 2 *UWB antenna to reject the notch bands*
(a) UWB-FN-FR4 antenna; (b) UWB-SN-FR4 antenna; (c) UWB-TN-FR4 antenna

2.3 Antenna Measurement in Bending Condition

The UWB-TN-FR4 antenna is bent on a Styrofoam cylinder as shown in Fig. 3. Measurement of the antennas in bending condition is performed on different diameters of Styrofoam cylinders ranging from 50 mm, 70 mm, 80 mm and 100 mm. The relative permittivity of the foam is 1.001 which is equal to the permittivity of air. This assumption is made based on the notion that antenna bends in free space without the proximity of the human body. The measured results of the bent antenna are compared with the antenna measured result under free space.

Table 2 *Dimensions of the two slots to notch the WiMAX, C- and WLAN bands*

Parameter	Values (mm)
L_e	4.6
W_e	11.9
L_f	5.6
W_f	4
L_h	3.9
W_h	1.5
W_3	1.8
W_4	0.5

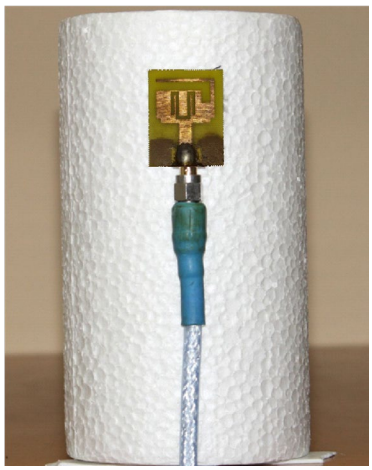

Fig. 3 UWB antennas' bent on styrofoam cylinder

3. Results and Analysis

In this section, the linear characteristics of the antennas on thin FR-4 substrate are presented to investigate the performance in terms of reflection coefficient, maximum surface current distributions, radiation patterns, gain, radiation efficiency, radiated power and bending condition. Furthermore, the SAR limit is simulated to satisfy the requirements enforced by the FCC and ICNIRP.

3.1 Reflection Coefficient

This section investigates the reflections coefficients of the UWB antennas in this work.

Int. Journal of Integrated Engineering Vol. 16 No. 1 (2024) p. 282-292

3.1.1 Fundamental UWB-FR4 Antenna

In this section, detailed results showing the resonance characteristic which is the reflection coefficient of the proposed UWB-FR4 antenna are discussed to show that the antenna has the desired result and operates effectively. The comparison between simulated and measured reflection coefficient of the UWB-FR4 antenna is shown in Fig. 4(a). The proposed antenna structure exhibits UWB resonance characteristics with satisfactory reflection coefficient. It is evident from the simulated reflection coefficient plot that within the UWB band, the proposed antenna possesses optimum impedance matching by achieving reflection coefficient less than -10 dB from 2.86 GHz to 11.78 GHz and yields an ultra-wide -10 dB impedance bandwidth. The maximum simulated reflection coefficient of the UWB-FR4 antenna is -36.45 dB, while the maximum measured reflection coefficient is -38 dB. Meanwhile, the measured reflection coefficient is greater than the -10 dB-line within a frequency range from 3 GHz until more than 12 GHz with a bandwidth of 9 GHz. It has also been reported in previous work that the operating frequencies of their UWB antennas exceeded 10.6 GHz [20]–[25]. This UWB-FR4 antenna does not possess signal rejection characteristics. It can be observed from the figure that the antenna has an optimum performance by covering the entire UWB frequency range and has a wideband resonance. Although fulfilling the requirements for good operation, the simulated and measured reflection coefficient curves have discrepancies. This may be due to the lossy properties of the substrate material which have a significant impact on the antenna's performance [26].

3.1.2 UWB-FN-FR4 Antenna

The simulated reflection coefficient obtained is compared with measured reflection coefficient as shown in Fig. 4(b) which specifies the notch characteristics of the antenna. The simulated reflection coefficient of the UWB-FN-FR4 antenna exhibits two UWB bandpass performance from 2.57 GHz to 3.20 GHz, and from 4.20 GHz to 12.15 GHz with an impedance bandwidth of 8580 MHz. A desired band notch covering the range from 3.20 GHz to 4.20 GHz has been achieved with a low reflection coefficient of -2.51 dB at mid-band frequency of 3.52 GHz and has a bandwidth of 1 GHz. The desired notch property is clearly achieved by incorporating the compact inverted L-shaped slot into the antenna structure. The measured reflection coefficient exhibits strong rejection at WiMAX and C- band from 3.15 GHz to 4.10 GHz, with a passband covering the UWB frequency band from 2.9 GHz up to more than 12 GHz. The measured result is in a good agreement with the simulated result. A slight deviation in higher frequencies might be due to substrate losses, measurement and fabrication errors [27]. Therefore, it is evident that a notch band corresponding to WiMAX and C-band frequencies is produced by adding the first slot.

3.1.3 UWB-SN-FR4 Antenna

The comparison between the simulation and measurement results of the reflection coefficient of the UWB-SN-FR4 antenna to notch the WLAN band is depicted in Fig. 4(c). The simulated impedance bandwidth extends from 2.84 GHz to 11.77 GHz with a rejection band from 5.12 GHz to 5.37 GHz, allowing for interference-free communication in the UWB system for the middle and upper ranges of the WLAN band as stipulated by the Malaysian Communications and Multimedia Commission (MCMC) [28], as required in this work. The reflection coefficient of band-notched structure also exhibits resonance at 7.5 GHz within the operating band. From the figure, the measured reflection coefficient is greater than the -10 dB-line throughout the UWB frequency range from 3.1 GHz to 10.6 GHz. The measured antenna can reject the upper frequency range of the WLAN band from 5.15 GHz to 5.40 GHz. The simulation result is in a good agreement with the measurement result. The performance of the simulated and measured reflection coefficient of the antenna demonstrates that the slot does introduce the desired notch property. The second slot of the UWB-SN-FR4 antenna has successfully blocked out the WLAN band and still performs good impedance-matching at other frequencies in the UWB band.

3.1.4 UWB-TN-FR4 Antenna

The reflection coefficient of the final design of the proposed UWB-TN-FR4 antenna are simulated and measured to show the triple notch bands characteristic of the antenna. Fig. 4(d) shows the comparison between the simulated and measured reflection coefficients results of the UWB-TN-FR4 antenna with a combination of two slots to notch the WiMAX, C- and WLAN bands. The simulated reflection coefficient of the antenna is below -10 dB from 2.51 GHz until 12.09 GHz and covers the entire UWB operation band. The first slot rejects the WiMAX band and C-band at the frequency from 3.17 GHz to 4.21 GHz with a reflection coefficient of -1.75 dB at mid-band frequency of 3.52 GHz. Meanwhile, the second slot rejects the WLAN band at the frequency from 5.13 GHz to 5.41 GHz with low reflection coefficient of -6.63 dB at mid-band frequency of 5.25 GHz. It is very clear that the desired notch bands are obtained by introducing both compact slots on the antenna's structure. The measured reflection coefficient has a wider UWB frequency range compared to the simulated reflection

coefficient. The response clearly reveals that there exists a rejection behavior for WiMAX and C-band from 3.1 GHz to 4.34 GHz and WLAN band from 5.04 GHz to 5.39 GHz. There is a slight frequency shift towards the higher frequencies in the measurement while rejecting the WiMAX, C-band and WLAN frequency bands.

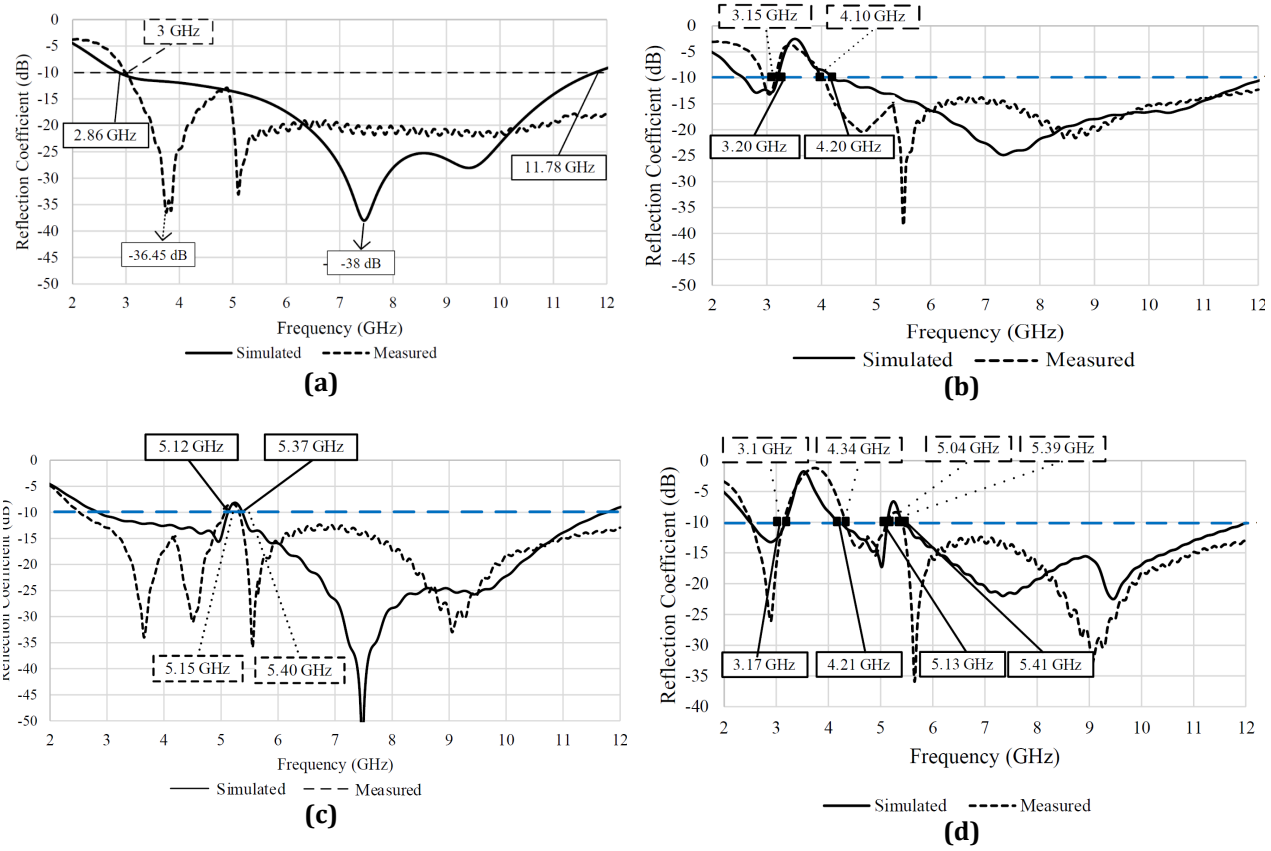

Fig. 4 *Comparison between the simulated and measured reflection coefficient of (a) UWB-FR4 antenna; (b) UWB-FN-FR4 antenna; (c) UWB-SN-FR4 antenna; UWB-TN-FR4 antenna*

3.2 Surface Current Distribution

The simulated surface current distribution on the UWB-TN-FR4 antenna at resonant frequencies of 3.1 GHz, 6.85 GHz and 10.6 GHz are shown in Fig. 5. At the lower frequency of 3.1 GHz, the maximum surface current is concentrated at the left portion of the first slot. Besides, the maximum surface current is also seen to be more distributed along the feed line and at the inner corner of the partial ground plane, indicating that these three structures aid in resonant frequency at lower frequencies. The maximum current remains along the sides of the feed line and partial ground plane as the frequency increases to 6.85 GHz. At the higher frequency of 10.6 GHz, small portions of the maximum surface current can be seen at the bottom edge of both arms of the second slot as well as at the lower region of the radiating patch, feed line and ground plane. As the maximum currents are concentrated along the feed line and inner corner of the partial ground plane in all three modes, the resonant frequencies clearly rely on these two structures to support multiple resonances across UWB operating frequency. Meanwhile, Fig. 6 shows the simulated surface current distribution at 3.52 GHz and 5.25 GHz notch bands. It is shown that the maximum surface currents are visible around the slot that is responsible for each notch band. Besides, the surface currents around the slots are in opposite directions on the right and left sides for both cases. As a result, radiation from one side currents will be canceled by the other side currents. Hence, no radiation or very low radiation occurs, and thus reflection coefficient of the antenna is lower at WiMAX, C-, and WLAN frequency bands and achieves triple band-notched characteristics [29].

Int. Journal of Integrated Engineering Vol. 16 No. 1 (2024) p. 282-292

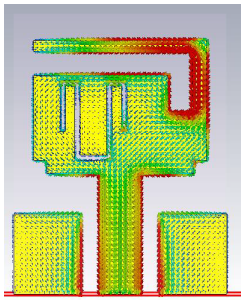

(a)

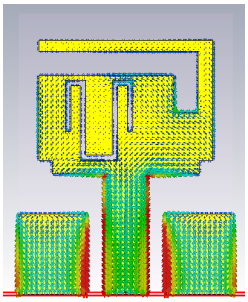

(b)

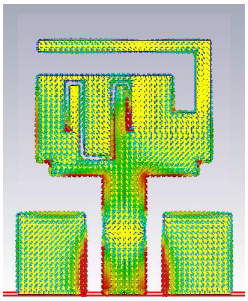

(c)

Fig. 5 *Simulated surface current distribution at (a) 3.1 GHz; (b) 6.85 GHz; (c) 10.6 GHz*

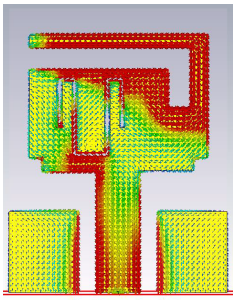

(a)

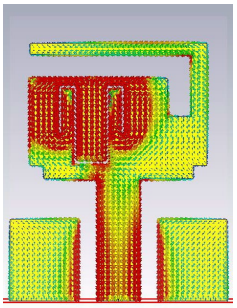

(b)

Fig. 6 *Simulated surface current distribution at (c) 3.52 GHz; (d) 5.25 GHz*

3.3 Radiation Pattern

The far-field radiation patterns in the E-plane of 2D and 3D of the antenna are studied and the simulated radiation patterns at UWB resonant frequencies of 3.1 GHz, 6.85 GHz and 10.6 GHz are shown in Fig. 7(a), Fig. 7(b) and Fig. 7(c) respectively. There is no specific application at each frequency, but rather the application as a whole UWB frequency range. One reference in particular [30], states that the application of UWB is concerning the 5G and IOT applications. At frequencies of 3.1 GHz and 6.85 GHz, the proposed antenna has a bidirectional radiation pattern in the E-plane with an eight-shaped pattern, In the higher frequency of 10.6 GHz, the radiation pattern slightly deteriorates in the E-plane, but still meets the requirements of UWB communication system. The UWB-TN-FR4 antenna has an omnidirectional pattern in the H-plane for all three frequencies, allowing it to send and receive signals in all directions [31].

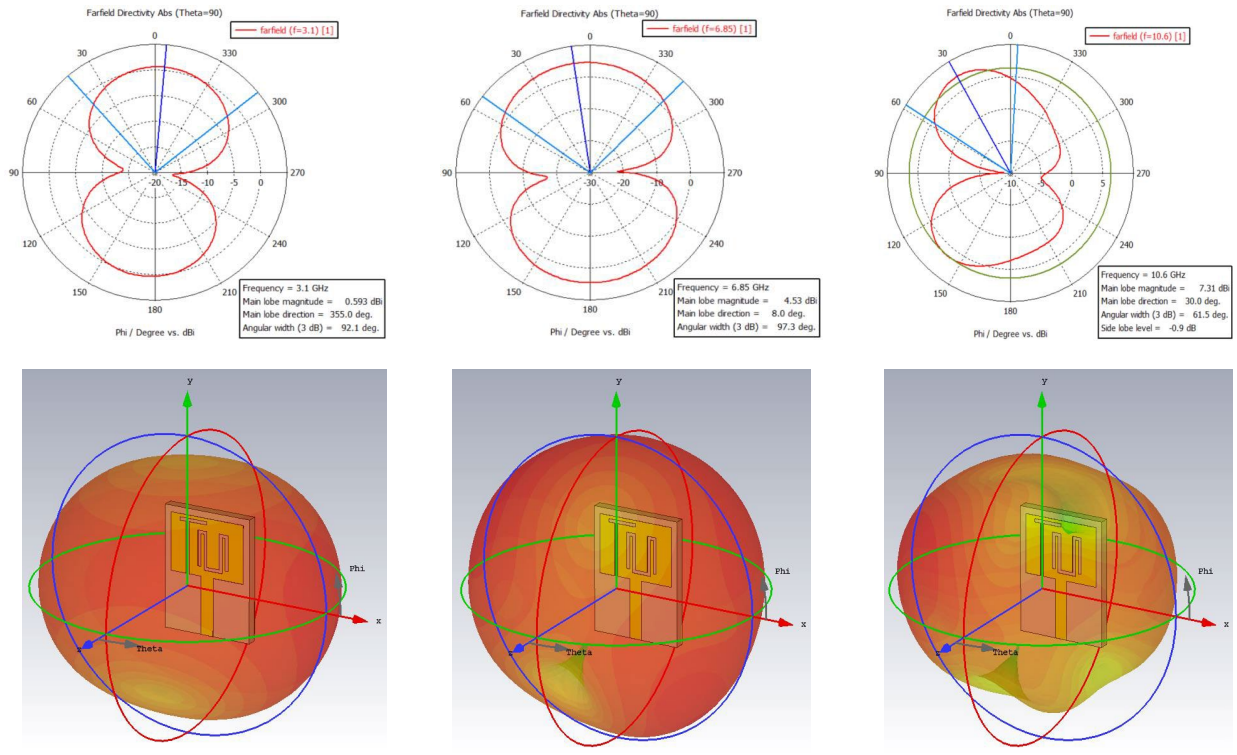

(a) (b) (c)

Fig. 7 *Radiation pattern of the UWB-TN-FR4 antenna in 2D and 3D at frequency (a) 3.1 GHz; (b) 6.85 GHz; (c) 10.6 GHz*

3.4 Gain, Radiation Efficiency and Radiated Power

The simulated gain and the radiation efficiency plots of the UWB-TN-FR4 antenna are shown in Fig. 8. The gain of the antenna varies from -8 dBi to 4 dBi across the UWB frequency. The low gain at the notch frequencies is observed which confirms the rejection of the three frequency bands. Meanwhile, the radiation efficiency of the proposed antenna fluctuates from approximately 0% to 100% over the UWB frequency range (3.1 GHz – 10.6 GHz) except at the notch bands. The sharp decrease in radiation efficiency which approaches 0% at both frequencies of 3.7 GHz and 5.25 GHz depicts that the antenna has poor radiation efficiency and does not radiate within the WiMAX, C- and WLAN rejection bands. Furthermore, the power radiation plot is shown in Fig. 9 which supports that there is no power radiated by the proposed antenna at the notch bands. All these responses support that the proposed UWB-TN-FR4 antenna is unresponsive for the signals transmitted over WiMAX, C- and WLAN systems.

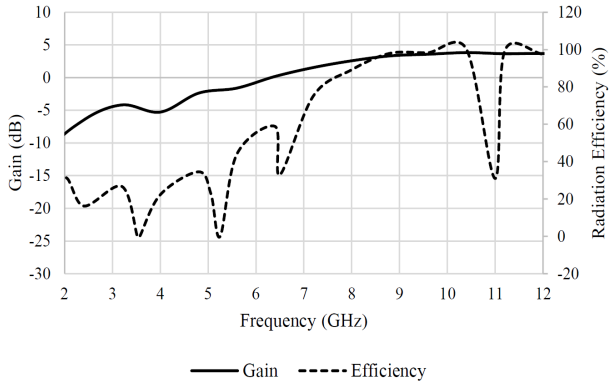

Fig. 8 *Simulated gain and radiation efficiency plots of the proposed UWB-TN-FR4 antenna*

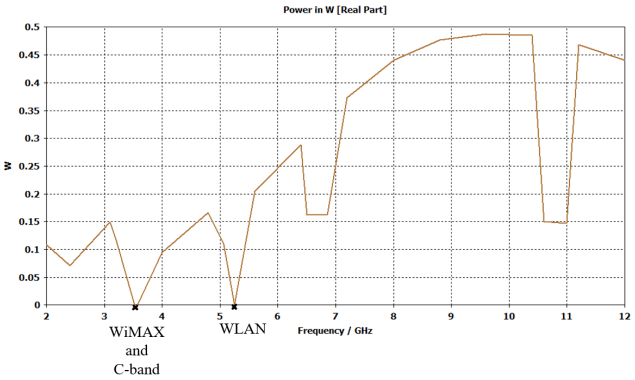

Fig. 9 *Simulated power radiation plot of the proposed UWB-TN-FR4 antenna*

3.5 Bending Investigation

Fig. 10 shows the measured reflection coefficient when the antenna is mounted on Styrofoam cylinders in free space with diameters of 50 mm, 70 mm, 80 mm and 100 mm, respectively. The proposed antenna covers the entire UWB band when it is mounted on non-flat surfaces. The impedance performance of the antenna is nearly identical for different bending angles except at 50 mm, where a small fluctuation is observed in the reflection coefficient at the third notch band frequencies. This is due to the severe bending condition, which changes the direction of the impedance transition. The reflection coefficient deteriorates slightly in the upper frequency band for all bending diameters but is maintained under -10 dB for the entire UWB band. Thus, the proposed UWB-TN-FR4 antenna can be mounted on a non-flat surface.

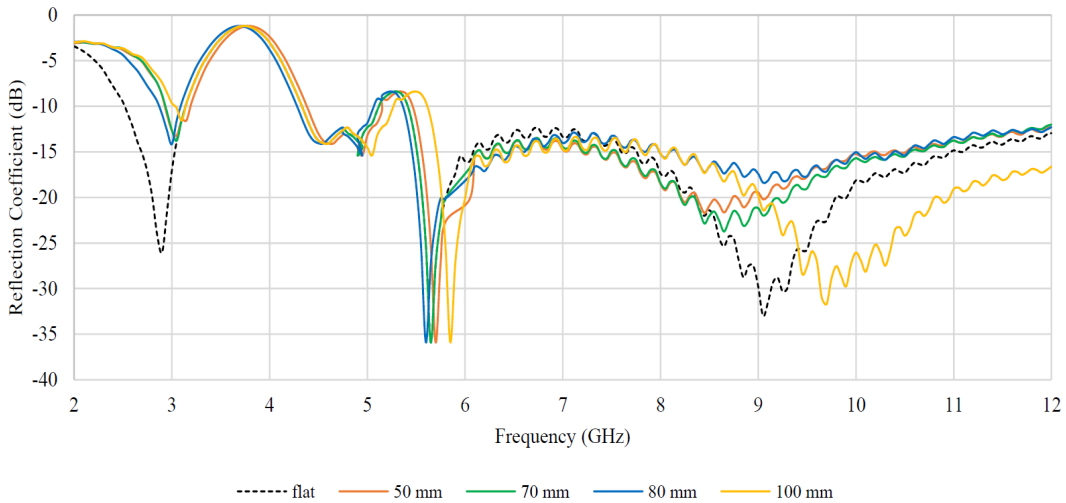

Fig. 10 *Measured reflection coefficient for different bending diameters of the UWB-TN-FR4 antenna*

Int. Journal of Integrated Engineering Vol. 16 No. 1 (2024) p. 282-292

3.6 Specific Absorption Rate (SAR) Analysis Through Validation

The SAR results for the UWB-TN-FR4 antenna are tabulated in Table 3. The SAR is simulated at three different UWB operating frequencies: 3.1 GHz, 6.85 GHz, and 10.6 GHz, and also at rejected frequencies: 3.52 GHz and 5.25 GHz for 1 g of human tissue with input power of 1 mW, 100 mW and 1 W. It is shown from the table that the SAR values are decreasing towards the higher frequencies because the dielectric properties of the human tissues are decreasing [32]. The SAR values of the antenna also decrease as the input power is reduced. Therefore, an input power of 1 mW is being considered as it yields the SAR values that adhere to the FCC and ICNIRP guidelines (1.6 W/kg over 1 g of human tissue). Fig. 11 depicts a comparison of SAR values with varying levels of input power. It can be seen that a 1 mW input power yields the SAR limits that comply with the FCC and ICNIRP guidelines for 1 g of human tissue for all three UWB resonant frequencies. Additionally, Table 4 shows the simulated SAR results for the UWB antenna at 10 g of human tissue when 1 mW of input power is used. The SAR limits have been shown to comply with the FCC and ICNIRP regulations, as they do not exceed 2 W/kg across the entire UWB frequency range which also includes the notch bands.

Table 3 *Simulated values of SAR with different input power for 1 g of human tissue*

	SAR values for 1 g of human tissue (W/kg) at different input power		
Input Power Frequency	**1 W**	**100 mW**	**1 mW**
3.1 GHz	9.356 W/kg	5.648 W/kg	1.586 W/kg
3.52 GHz	3.870 W/kg	1.515 W/kg	1.024 W/kg
5.25 GHz	2.983 W/kg	1.256 W/kg	0.877 W/kg
6.85 GHz	4.059 W/kg	1.546 W/kg	1.215 W/kg
10.6 GHz	1.492 W/kg	0.971 W/kg	0.924 W/kg

Table 4 *Simulated SAR values at three resonant frequencies for 10 g human tissue with 1 mW input power*

Frequency	Total SAR (W/kg)
3.1 GHz	0.153
3.52 GHz	0.057
5.25 GHz	0.013
6.85 GHz	0.022
10.6 GHz	0.088

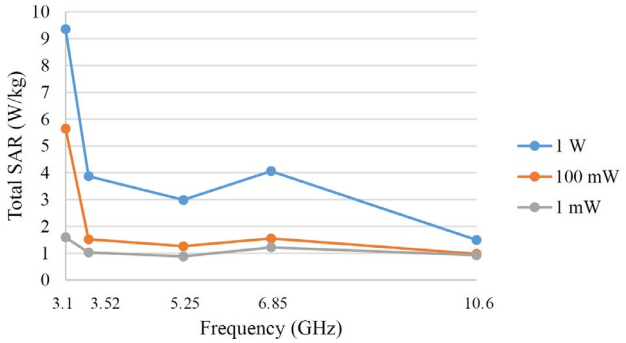

Fig. 11 *Simulated SAR results of UWB-TN-FR4 antenna with different values of input power*

4. Conclusion

A compact UWB-TN-FR4 antenna with triple band-notched characteristics has been designed, simulated and fabricated. Two slots are introduced on the radiating patch of the microstrip antenna to generate the WiMAX, C- and WLAN notch bands. The antenna is fabricated on a thin FR-4 substrate with dielectric constant, εr of 4.5, loss tangent, tan δ of 0.019 and thickness, h of 0.5 mm. The antenna exhibits a -10 dB bandwidth of 3.1 GHz until 10.6 GHz, proving it is able to operate over the UWB frequency with sharp band notches from the WiMAX and C-band from 3.17 GHz to 4.21 GHz (actual WiMAX band: 3.2 GHz to 3.7 GHz; actual C-band: 3.7 GHz to 4.2 GHz) and the WLAN system at 5.13 GHz to 5.41 GHz (actual WLAN band: 5.15 GHz to 5.35 GHz). The antenna shows satisfactory omnidirectional radiation characteristics throughout its operating band with a maximum simulated peak gain of 4 dBi. The proposed structure also shows high radiation efficiency up to 100% which is one of the most desirable features of UWB antenna. The performance of the antenna is not affected under bending conditions with different diameters of 50 mm, 70 mm, 80 mm and 100 mm, which represents approximately different sizes of human arm. The SAR results obtained shows that the UWB antenna triple notch bands obey the guidelines for 1 mW input power for 1 g and 10 g of human tissue. This antenna has a stable frequency response with wideband resonance, satisfactory gain and radiation characteristics that are suitable for wearable wireless communication. The comparison shows that the simulated and measured reflection coefficients are in a good agreement with each other.

Acknowledgement

This work was supported by the Ministry of Higher Education (MoHE) under Fundamental Research Grant Scheme FRGS/1/2020/TK0/UTHM/02/44.

Conflict of Interest

Authors declare that there is no conflict of interests regarding the publication of the paper.

Author Contribution

The authors confirm contribution to the paper as follows: ***study conception and design:*** *M. A. A. Rashid, S. M. Shah;* ***data collection:*** *M. A. A. Rashid;* ***analysis and interpretation of results:*** *M. A. A. Rashid;* ***draft manuscript preparation:*** *S. M. Shah, H. A. Majid, U. Musa, N. S. Suriani. All authors reviewed the results and approved the final version of the manuscript.*

References

[1] Hall, P. S., Hao, Y., Nechayev, Y. I., Alomainy, A., Constantinou, C. C., Parini, & Bozzetti, M. (2007). Antennas and propagation for on-body communication systems. *IEEE Antennas and Propagation Magazine*, *49*(3), 41-58.

[2] Alemaryeen, A., & Noghanian, S. (2019). On-body low-profile textile antenna with artificial magnetic conductor. *IEEE Transactions on Antennas and Propagation*, *67*(6), 3649-3656.

[3] Gao, G. P., Hu, B., Wang, S. F., & Yang, C. (2018). Wearable circular ring slot antenna with EBG structure for wireless body area network. *IEEE Antennas and Wireless Propagation Letters*, *17*(3), 434-437.

[4] Alomainy, A., Sani, A., Rahman, A., Santas, J. G., & Hao, Y. (2009). Transient characteristics of wearable antennas and radio propagation channels for ultrawideband body-centric wireless communications. *IEEE Transactions on Antennas and Propagation*, *57*(4), 875-884.

[5] Liu, H. W., Ku, C. H., Wang, T. S., & Yang, C. F. (2010). Compact monopole antenna with band-notched characteristic for UWB applications. *IEEE Antennas and wireless propagation letters*, *9*, 397-400.

[6] Chandel, R., & Gautam, A. K. (2016). Compact MIMO/diversity slot antenna for UWB applications with band-notched characteristic. *Electronics Letters*, *52*(5), 336-338.

[7] Bashiri, M., Ghobadi, C., Nourinia, J., & Majidzadeh, M. (2017). WiMAX, WLAN, and X-band filtering mechanism: Simple-structured triple-band frequency selective surface. *IEEE Antennas and Wireless Propagation Letters*, *16*, 3245-3248.

[8] IEEE P802.15 Working Group for Wireless Personal Area NetworkTG6 . "Body area networks." (2013). http://www.ieee802.org/15/pub/TG6.htm.

[9] Trajkovikj, J., & Skrivervik, A. K. (2016, April). Comparison of SAR of UHF wearable antennas. In 2016 10th European Conference on Antennas and Propagation (EuCAP) (pp. 1-4). IEEE.

[10] MS492:522 (1999). Guidelines for limiting exposure to time-varying electric, magnetic and electromagnetic fields (up to 300 GHz). ICNIRP

[11] Xu, F., Chen, X., & Wang, X. A. (2012). UWB antenna with triple notched bands based on folded multiple-mode resonators. IEICE Electronics Express, 9(11), 965-970.

[12] Sarkar, D., Srivastava, K. V., & Saurav, K. (2014). A compact microstrip-fed triple band-notched UWB monopole antenna. IEEE Antennas and Wireless Propagation Letters, 13, 396-399.

[13] Balani, W., Sarvagya, M., Ali, T., Samasgikar, A., Das, S., Kumar, P., & Anguera, J. (2021). Design of SWB antenna with triple band notch characteristics for multipurpose wireless applications. Applied Sciences, 11(2), 711.

[14] Kumar, G., & Kumar, R. (2019). A survey on planar ultra-wideband antennas with band notch characteristics: Principle, design, and applications. AEU-International Journal of Electronics and Communications, 109, 76-98.

[15] Abdul Rashid, M. A. Z., Mohd Shah, S., & Ponniran, A. (2019). A compact triple-notch band ultra-wideband antenna. Universal Journal of Electrical and Electronic Engineering, 6(5H), 55-66.

[16] Alotaibi, S., & Alotaibi, A. A. (2020). Design of a planar tri-band notch UWB antenna for X-band, WLAN, and WiMAX. Engineering, Technology & Applied Science Research, 10(6), 6557-6562.

[17] Sanyal, R., Sarkar, P. P., & Sarkar, S. (2019). Octagonal nut shaped monopole UWB antenna with sextuple band notched characteristics. AEU-International Journal of Electronics and Communications, 110, 152833.

[18] Cui, L., Liu, H., Hao, C., & Sun, X. (2019). A novel UWB antenna with triple band-notches for WiMAX and WLAN. Progress In Electromagnetics Research Letters, 82, 101-106.

[19] Puri, S. C., Das, S., & Tiary, M. G. (2020). UWB monopole antenna with dual-band-notched characteristics. Microwave and Optical Technology Letters, 62(3), 1222-1229.

[20] Garg, R. K., Nair, M. V. D., Singhal, S., & Tomar, R. (2021). A miniaturized ultra-wideband antenna using "modified" rectangular patch with rejection in WiMAX and WLAN bands. Microwave and Optical Technology Letters, 63(4), 1271-1277.
[21] Abbas, A., Hussain, N., Lee, J., Park, S. G., & Kim, N. (2020). Triple rectangular notch UWB antenna using EBG and SRR. IEEE Access, 9, 2508-2515.
[22] Rekha, V. S. D., Pardhasaradhi, P., Madhav, B. T. P., & Devi, Y. U. (2020). Dual band notched orthogonal 4-element MIMO antenna with isolation for UWB applications. IEEE Access, 8, 145871-145880.
[23] Park, S., & Jung, K. Y. (2022). Novel compact UWB planar monopole antenna using a ribbon-shaped slot. IEEE Access, 10, 61951-61959.
[24] Khan, M. M., & Sultana, A. (2020). Novel and compact ultra-wideband wearable band-notch antenna design for body sensor networks and mobile healthcare system. Engineering Proceedings, 3(1), 1.
[25] Mahmood, S. N., Ishak, A. J., Jalal, A., Saeidi, T., Shafie, S., Soh, A. C., ... & Abbasi, Q. H. (2021). A Bra Monitoring System Using a Miniaturized Wearable Ultra-Wideband MIMO Antenna for Breast Cancer Imaging. Electronics, 10(21), 2563.
[26] Ashyap, A. Y., Dahlan, S. H., Abidin, Z. Z., Kamarudin, M. R., Majid, H. A., Alduais, N. A. M., ... & Alhandi, S. A. (2021). C-shaped antenna based artificial magnetic conductor structure for wearable IoT healthcare devices. Wireless Networks, 27, 4967-4985.
[27] Arora, S., Sharma, S., & Rana, A. K. (2022). Ultrawide Band Antenna for Wireless Communications: Applications and Challenges. Internet of Things, 95-106.
[28] 1:15 (2013). Guideline on the Provision of Wireless Local Area Network (WLAN) Service. Malaysian Communications and Multimedia Commission.
[29] Tang, Z., Wu, X., Zhan, J., Hu, S., Xi, Z., & Liu, Y. (2019). Compact UWB-MIMO antenna with high isolation and triple band-notched characteristics. IEEE access, 7, 19856-19865.
[30] Ashyap, A. Y., Dahlan, S. H. B., Abidin, Z. Z., Abbasi, M. I., Kamarudin, M. R., Majid, H. A., ... & Alomainy, A. (2020). An overview of electromagnetic band-gap integrated wearable antennas. IEEE Access, 8, 7641-7658.
[31] Cho, Y. J., Kim, K. H., Choi, D. H., Lee, S. S., & Park, S. O. (2006). A miniature UWB planar monopole antenna with 5-GHz band-rejection filter and the time-domain characteristics. IEEE Transactions on Antennas and Propagation, 54(5), 1453-1460.
[32] Yin, B., Gu, J., Feng, X., Wang, B., Yu, Y., & Ruan, W. (2019). A low SAR value wearable antenna for wireless body area network based on AMC structure. Progress In Electromagnetics Research C, 95, 119-129.